Published in final edited form as:
Acta Biomater. 2012 October ; 8(10): 3596–3605. doi:10.1016/j.actbio.2012.06.013.

Thermoresponsive nanogels for prolonged duration local anesthesia

Todd Hoare[1], **Stuart Young**[1], **Michael W. Lawlor**[2], and **Daniel S. Kohane**[3,*]

[1]Department of Chemical Engineering, McMaster University, 1280 Main St. W, Hamilton, Ontario, Canada L8S 4L7

[2]Department of Pathology and Laboratory Medicine, Children's Hospital of Wisconsin and Medical College of Wisconsin, Milwaukee, WI, 53226

[3]Laboratory for Biomaterials and Drug Delivery, Department of Anesthesiology, Division of Critical Care Medicine, Children's Hospital Boston, Harvard Medical School, 300 Longwood Ave., Boston, MA , U.S.A. 02115

Abstract

Nanogels based on poly(N-isopropylacrylamide) are attractive vehicles for prolonged duration local anesthesia because of their tunable size, number of functional groups, thermoresponsiveness, and their anionic charge. Nerve block durations of up to nine hours were achieved using acrylic acid-loaded nanogels loaded with bupivacaine. Increasing the anionic charge density of the nanogels or (for more highly acid-functionalized nanogels) decreasing the nanogel size facilitated longer duration anesthetic release. Small (<300 nm diameter) nanogels formed dense aggregates upon injection *in vivo* and induced only mild inflammatory responses, while large (>500 nm diameter) nanogels typically remained as liquid-like residues *in vivo* and induced more severe inflammatory reactions.

Keywords

nanogels; poly(N-isopropylacrylamide); nerve block; local anesthesia; drug delivery

1. INTRODUCTION

Prolonged duration local anesthesia after surgery is a significant current clinical need. To meet this goal, bioerodible polymer implants[1, 2], liposomes[3–5], degradable microparticles[6–11], hydrogels[12–15], viscous polymer formulations[16], drug-grafted polymer solutions[17], or combinations thereof[18, 19] have all been applied as drug delivery vehicles for local anesthetics. In most cases, injectable systems for local anesthetic delivery are successful in prolonging local anesthesia over the course of several hours relative to injections of the anesthetic solution alone, although the use of synergistic drug combinations may extend this time period to several days[5].

*To whom correspondence should be addressed Dr. Daniel Kohane, Farley 605, Children's Hospital Boston, 300 Longwood Avenue Boston, MA 02114, Tel: 1-617-355-7327, Fax: 1-617-730-0453, Daniel.Kohane@childrens.harvard.edu.

Nanogels, sub-micron hydrogel particles with colloidal properties, are interesting candidates as drug delivery vehicles because the hydrogel nanostructure of nanogels can be engineered to achieve controlled pore structures, chemical topologies, and swelling responses to environmental stimuli[20], while the colloidal nanoparticle macrostructure of nanogels offers the advantages of high specific surface areas and ready injectability. Thermosensitive nanogels based on poly(N-isopropylacrylamide) (PNIPAM) offer the further potential advantage of undergoing a volume phase transition as they are heated above a critical temperature, resulting in significant gel deswelling and (in some cases) thermally-triggered aggregation of the nanogel particles to form aggregates and/or physically-crosslinked hydrogels[21]. Since thermosensitive nanogels can exhibit triggerable changes in pore size and colloidal stability, they have been widely investigated for the “on-demand” delivery of drugs or model drugs including acetylsalicylic acid[22], fluorescein-labelled dextran[23], insulin[24], and bovine serum albumin[25], among others. *In vitro* drug release has also been demonstrated from macroscopic assemblies of nanogels, including polyelectrolyte-assembled nanogel thin films[26, 27], surface-grafted nanogel monolayers[28], and bulk hydrogels comprised of crosslinked nanogel particles[29].

Functionalized thermoresponsive nanogels could be particularly effective for controlling the release of local anesthetics, which are generally cationic, given the ease of functionalizing nanogels with high concentrations of anionic groups (enhancing the affinity between the drug and the nanogel phase) and the potential application of the thermal phase transition to induce nanogel aggregation to localize nanogels at a desired site. The ability of anionically-functionalized PNIPAM nanogels to bind and release cationic drugs (such as commercially available anesthetics) has been demonstrated [30, 31]. We have also previously shown the potential of PNIPAM-based nanogels as highly effective binding agents and/or scavengers for bupivacaine, a common local anesthetic[32]. Here, we investigate the capacity of nanogels to facilitate controlled release of bupivacaine to provide long-term local anesthesia, using a rat sciatic nerve animal model to assay the *in vivo* performance of nanogel drug delivery formulations.

2. MATERIALS AND METHODS

2.1 Materials

N-isopropylacrylamide (NIPAM, 99%), acrylic acid (AA, 99%), dimethylaminoethyl acrylate (DMAEA, 99%), N,N-methylenebisacrylamide (BIS, 99%), sodium dodecyl sulfate (SDS, 99.5%), bupivacaine hydrochloride (bupivacaine, 99%), and bovine serum albumin (BSA, 96%) were purchased from Sigma-Aldrich and used as received. Ammonium persulfate (APS, 99%) was purchased from Fluka. Sterile saline for injections (0.15M NaCl) was purchased from Baxter Pharmaceuticals. Phosphate buffered saline (PBS, 20mM buffer, 0.15M ionic strength) was purchased from Invitrogen. All water used in the synthesis and purification was of Milli-Q grade.

2.2 Nanogel Synthesis

Nanogels were prepared as previously described[32]. Briefly, all required monomers and surfactants were dissolved in 150 mL water inside a 500 mL round-bottom flask and heated to 70°C under a N_2 purge and 200 RPM magnetic mixing. After 30 minutes, 0.10 g of APS was dissolved in 5 mL water and injected into the reactor to initiate polymerization. After four hours of reaction, the nanogels were cooled, purified over 8 cycles of dialysis using a 500 kDa MWCO poly(vinylidene fluoride) membrane, and lyophilized for storage. Note that no significant turbidity changes are observed after 30-40 minutes of reaction time, suggesitng the nanogels are largely formed by this time.

The recipes used to synthesize the nanogels for this work are summarized in Table 1 together with the particle size and electrophoretic mobility of the resulting nanogels, measured in PBS at 25°C. Nanogel particle size was measured using a Zeta Plus dynamic light scattering instrument operating at 90° (Brookhaven Instruments Inc.) while nanogel electrophoretic mobility was measured using the Zeta Plus instrument (Brookhaven Instruments Inc.) operating in phase analysis light scattering mode. The nanogel codes represent the type of functional monomer used to prepare the nanogel (AA or DMAEA), the mole percentage of functional monomer used to prepare the nanogel (6 mol%, 20 mol%, or 33 mol%), and the relative size of the nanogel (S = small, M = medium, L = large).

2.3 In Vitro Cytotoxicity Evaluation

A MTT assay was used to evaluate the biocompatibility of the nanogels with mouse-derived C2C12 myoblasts (cultured in Invitrogen DMEM medium supplemented with 10% fetal bovine serum and 1% penicillin streptomycin), mouse-derived 3T3 fibroblasts (cultured in ATCC DMEM medium supplemented with 10% calf serum albumin and 1% penicillin streptomycin), and mouse-derived J.1774 macrophage-like cells (cultured in Invitrogen DMEM medium supplemented with 10% fetal bovine serum and 1% penicillin streptomycin). Each cell line was plated in 1mL aliquots in a 24-well plate at a density of 30,000 cells/well and permitted to adhere and stabilize over 24 hours. For differentiating myoblasts into myotubes, the FBS growth medium was replaced with 2% horse serum and 1% penicillin streptomycin-supplemented DMEM media and cultured an additional eight days prior to material addition, with regular media changes every 3 days. Cell culture passages 3-35 were used for biocompatibility studies. Materials were sterilized as dry powders under a UV lamp over three hours. Nanogels were resuspended in sterile 0.9% saline under gentle mixing at the desired concentration. 0.1mL aliquots of nanogels (materials wells) or sterile saline (control wells) were then added to cultured cells. Four replicate wells were tested for each material together with media-only and cell-only controls. At time points of 24 hours and 4 days after material addition, both the media and the test material was removed and replaced with 1 mL of fresh media and 100 μL of MTT reagent. Solubilization solution (Promega) was added after four hours of incubation and the plates were mixed on an orbital stirrer for 24 hours. The absorbances of each of the wells were then measured in duplicate in a 96-well plate using a multi-well plate reader (Molecular Devices) operating at 570 nm. Results were baseline-corrected to eliminate the impact of media absorbance and are normalized relative to the cell-only results. Reported cell viabilities represent averages of four repeat experiments, with errors representing the standard deviation of the replicates.

2.4 In Vivo Nerve Blocks

Young adult male Sprague-Daley rats with weights ranging between 350-450 g were purchased from Charles River Laboratories (Wilmington, MA) and housed in pairs using a 7AM-7PM light-dark cycle. Animals were cared for in compliance with protocols approved by the Animal Care and Use Committee at the Massachusetts Institute of Technology. NIH guidelines for the care and use of laboratory animals (NIH Publication #85-23 Rev. 1985) have been observed. Each rat was injected only once to ensure the blockade effect was attributable exclusively to the tested formulation.

Rats were briefly (< 2 minutes) anesthetized with isofluorane in 100% oxygen prior to injection. A 25G needle was introduced postero-medial to the greater trochanter, pointing in an anteromedial direction. Upon contact with the bone, 0.3 mL of a nanogel suspended in a bupivacaine solution was injected into the left leg of the rat. Nanogel concentrations ranging from 20-160 mg/mL and bupivacaine concentrations ranging from 5-15 mg/mL were evaluated, all prepared in sterile saline. Nanogels were also injected without drug at the

same concentrations to assess the tissue biocompatibility of the nanogels; no effective nerve blocks were achieved upon nanogel injection in the absence of bupivacaine for any of the compositions tested. The right leg was used as a control. Both sensory and motor block were evaluated at half hour time points by a blinded experimenter for the first 1.5 hours of the block and 45 minute time points for the remainder of the block. Two data points were also obtained after the completion of the nerve block, one on the next scheduled time point of the test and the other 24 hours post-injection, to ensure complete recovery of normal neurological function. Sensory blocks were evaluated using a modified hotplate test, while motor block was assessed by measuring the weight each animal could bear on a single leg[9, 33]. Four rats were analyzed for each treatment; animals only participated in one experiment. Durations of nerve block durations are represented as means with standard deviations.

2.5 Rat Sciatic Nerve Dissection

Rats were sacrificed one and four days post-injection. The thermoaggregation of nanogels *in vivo* was assessed by qualitative inspection of the nanogel residue in the nanogel 1 day post-injection. Adhesions within the tissue were qualitatively scored on the scale 0 = no adhesion, 1 = weak adhesion easily separated by low forces, 2 = moderate adhesion separable by gentle dissection, 3 = strong adhesion separable only by blunt dissection. The sciatic nerve was removed together with surrounding tissues[35] by a blinded dissector (TH) and placed immediately in Accustain formalin-free fixative. The nerve was sectioned and stained with hematoxylin-eosin to prepare histology slides using standard techniques. Slides were analyzed by an observer (MWL) blinded to the nature of the material injected into the animal being observed.

2.6 In vitro Nanogel Aggregation Assays

Aggregation temperatures of nanogels were measured by suspending nanogels at concentrations between 1 mg/mL to 80 mg/mL in saline (0.15M NaCl), both in the presence and absence of 0.1mM BSA. This BSA concentration was chosen to mimic the approximate protein concentration in interstitial fluid[34]. Starting at 20°C, the temperature of the suspensions was ramped up at intervals of 5°C, with a ten minute wait time between temperature steps. Aggregation temperatures were tracked both visually (all samples formed discrete, macroscopic aggregates at a narrow temperature range) and by UV/VIS spectrophotometry (by the rapid increase in transmission as the aggregates settle). Once the rough aggregation temperature was identified, smaller temperature step experiments were performed to identify the precise aggregation temperature (0.2°C) using the same methods. Four replicates were performed to confirm the reproducibility of the aggregation transition, with the reported results representing the average of the four replicates.

2.7 Statistical Methods

Cytotoxicity data are presented as means with standard deviations. The durations of nerve blockade from *in vivo* neurobehavioral testing are expressed as means with standard deviations. Comparisons between sensory and motor blocks for a given group are made using a paired t-test while those between different groups are made using unpaired t-tests. Linear regressions and t-tests are performed using Microsoft Excel.

3. RESULTS

3.1 Nanogel Characterization

The nanogels synthesized for this study ranged in size from ~100 nm to ~1 μm with functional monomer loadings ranging from 6 mol% to 33 mol% acrylic acid (AA) or dimethylaminoethyl methacrylate (DMAEA), as shown in Table 1. Each nanogel tested

exhibited a low polydispersity (<0.01) by dynamic light scattering, such that the particles can all be considered essentially monodisperse. For each acrylic acid loading tested, nanogels were synthesized in the size ranges 800–1000 nm ("large", L), 250–450 nm ("medium", M), and 100-200 nm ("small", S) in order to decouple the effects of nanogel size and nanogel functionalization on the observed durations of nerve block. Note that each of the tested nanogels were at least 96% ionized at pH 7.4 (Supplementary Data, Figure S1), such that the functional group content and the charge content of the nanogels can be considered equal. Nanogels with higher degrees of functionalization had higher average pK_a values (Supplementary Data, Figure S2), as anticipated based on the polyelectrolyte effect. The cationic DMAEA nanogel had a comparable size to the "small" acrylic acid-functionalized nanogels, making it a useful control to evaluate the impact on drug delivery of the type of functional group incorporated into the nanogel. The DMAEA-functionalized nanogel exhibited a negative net charge in the zeta potential measurement in PBS due to divalent counterion condensation on the surface of the nanogel; a cationic charge (+0.22 x 10^{-8} m^2/Vs) was measured in a 1mM NaCl solution. The nomenclature of the particles is: TYPE-NN-SIZE, where TYPE is the functional group, NN is the % functional group loading, and the SIZE is S, M, or L (corresponding to the size ranges defined above).

3.2 Cytotoxicity

To confirm the potential utility of nanogels for drug delivery *in vivo*, nanogel cytotoxicity was assayed using 3T3 mouse fibroblasts, J1774 macrophage-like cells, and C2C12 mouse myoblasts in cell culture (Figure 1). Nanogels had minimal impact on cell viability after 1 and 4 days of exposure, although nanogels with lower degrees of acid functionalization maintained slightly higher cell viability than those with higher degrees. For example, cell viability in the presence of AA-6L was higher than that of AA-20L for fibroblasts (p = 0.02), macrophages (p = 0.006), and myoblasts (p = 0.0004) despite the similar particle size of both nanogels. This difference may be related to the particle itself and/or the acidity of the non-buffered nanogel suspension in saline added to the cell wells. Indeed, due to the highly acidic nature of the AA-20 and AA-33 nanogels tested (pH~3.5 when suspended in saline), the media changed in color from red to light orange when 2 mg/mL nanogel was added. Such local acidity might be neutralized *in vivo*, where there is continuous fluid turnover. Indeed, no significant myotoxicity was observed even when a 40-fold higher concentration of nanogels was administered *in vivo* (see section 3.3). Nanogels functionalized with the same percentage of the basic comonomer DMAEA (DMAEA-20) exhibited no significant cytoxicity for any cell type.

Particle size also had a mild impact on nanogel cytotoxicity in nanogels with high acid functionalization. While AA-6L and AA-6S did not exhibit significantly different cytotoxicity with any cell type (p > 0.06), AA-20L exhibited slightly higher cytotoxicity to myoblasts (p = 0.0008) compared to AA-20S despite having an equivalent number of –COOH groups. Neither macrophages (p = 0.41) nor fibroblasts (p = 0.06) showed a significant sensitivity to particle size, even with the AA-20 nanogels. From the above result, particle size had a minor influence on cytotoxicity for more highly functionalized nanogels, but the acidity of the nanogels seemed to have a greater effect. Nonetheless, cytotoxicity was relatively minor in all cases, suggesting that the nanogels are appropriate for use *in vivo*.

3.3 Tissue Response

Figure 2 shows the tissue response four days after injection of a 80 mg/mL suspension of blank (no drug) AA-6 nanogels of different sizes at the rat sciatic nerve. Injection of the large, 840 nm nanogels (AA-6L) induced an extensive inflammatory response resulting in the formation of a thick inflammatory capsule (Figure 2(a) inset) around a white, low

viscosity residue (volume 0.2 – 0.3 mL) consistent with the properties of the original injected nanogel suspension. Significant matting of the tissues (tissues stuck to each other, planes difficult to separate) was also observed, with score 3 adhesions (see Methods) noted between the inflammatory complex and the surrounding tissue and significant local bleeding observed upon dissection due to increased vascularization around the inflammatory complex. This complex persisted up to at least one month post-injection (data not shown). In contrast, when the nanogel size was reduced to 265 nm (AA-6M), a dense, gel-like deposit was recovered that consisted of a mixture of nanogels and inflammatory cells according to histological analysis. Score 1 adhesions were observed between the gel deposit and the surrounding tissues, and no significant bleeding occurred upon dissection. When nanogel size was further reduced to 100 nm (AA-6S), no nanogel deposit whatsoever was observed upon dissection. No adhesions or tissue matting were observed between the injection site and the surrounding tissues, with the tissues visually appearing similar to pristine tissue.

A similar trend was observed with the AA-20 nanogels, as shown in Figure 3. The large AA-20L nanogels remained as a suspension and induced formation of a thick capsule around the suspended gel after 4 days. After 14 days, the inflammatory complex persisted but the liquid nanogel suspension observed inside the complex after four days became a solid, gel-like inner core, a condition which persisted at least one month post-injection (data not shown). The area around the injection was highly vascularized and matted, with score 2–3 adhesions consistently observed. The smaller AA-20S nanogels showed a small aggregate on the nerve after 4 days and complete resorption of the aggregate after 2 weeks. No significant adhesions or visual signs of inflammation were observed at either time point for AA-20S.

With AA-33 nanogels, the general trend observed with AA-6 and AA-20 nanogels was again seen, with large nanogels inducing a large apparent inflammatory response while small nanogels induced less inflammation (Supplementary Data, Figure S3). However, in contrast to the AA-6 and AA-20 results, no free-flowing suspension was found inside the inflammatory capsule in AA-33L; instead, the residue was gel-like in nature, similar to residues observed for the smaller nanogels.

Histological analysis of hematoxylin and eosin-stained paraffin-embedded sections of tissue confirmed that the apparent differences in inflammation between large and small nanogels observed visually during dissections reflected differences in tissue reaction. Figure 4 shows representative histology four days after injection for AA-20S (Fig. 4a) and AA-20L (Fig. 4b). At this time point, some minimal degree of inflammatory response and granulation tissue formation is normal in the area of the injection due to post-surgical wound healing; these findings were seen to a variable extent for all nanogels, but would not account for the different degrees of inflammation seen with different nanogel injections. AA-20S nanogels (particle size ~200 nm, Fig. 4a) produced a typical inflammatory response at the site of injection consisting of lymphocytes and macrophages that was restricted to the surface of the muscle and the surrounding fibroadipose tissue, with minimal infiltration into muscle tissue. In contrast, AA-20L nanogels (particle size ~1000 nm, Fig. 4b) elicited a considerably greater inflammatory response, both in terms of the area affected by the inflammation and the degree to which muscle infiltration occurred. Given the identical injection volumes, total nanogel masses administered, and chemical compositions of AA-20S and AA-20L, these findings suggest that nanogel size is a major determinant of the tissue response to implantation, with small nanogels exhibiting a significantly lower inflammatory response. No significant difference in inflammation was noted between nanogels with similar sizes but different acrylic acid loadings.

Injection of the DMAEA-functionalized nanogels (particle sizes 145–245 nm at 37°C) yielded similar biological responses to the small AA-20 and AA-6 nanogels, with zero adhesions, zero residual nanogel, and no significant inflammation or adhesions observerable four days post-injection. Histological analysis indicated only minor inflammation similar to that observed for small acrylic acid-functionalized nanogels. .

3.4 Duration of Nerve Block

Nanogels (80 mg/mL) suspended in 5 mg/mL bupivacaine solution were injected at the sciatic nerve and the duration of nerve blockade was measured, with the results of both latency and motor blocks as well as the thermoaggregation temperature observed *in vitro* for each nanogel tested shown in Table 2. DMAEA-20 nanogels, which contained cationic monomers (i.e. the same charge as bupivacaine) achieved nerve block durations which were not significantly longer than that achieved via injection of a 5mg/mL bupivacaine solution without nanogels ($p = 0.14$), despite the high (20 mol%) degree of functionalization of these nanogels. This result suggests that drug does not partition within the DMAEA nanogels, resulting in unchanged release kinetics versus a simple bupivacaine solution injection. In contrast, acrylic acid-functionalized nanogels (which were largely ionized at pH 7.4 and thus contained a net anionic charge and ionic binding sites for cationic bupivacaine) significantly increased the duration of block to a degree related to the number of $–COO^-$ groups in the nanogel. AA-6 nanogels of all sizes achieved higher durations of nerve block than bupivacaine-only injections ($p = 0.005$ for AA-6L, $p = 0.0007$ for AA-6M, and $p = 0.001$ for AA-6S). Correspondingly, AA-20 nanogels of all sizes exhibited longer durations of block than AA-6 nanogels of the same size ($p = 0.002$ for pair-wise comparisons in all cases). Based on previous studies of bupivacaine-nanogel binding[32], the presence of more $–COO^-$ groups in the nanogel phase promotes more and stronger interactions between the nanogel and cationic bupivacaine, retarding drug release.

Particle size had no significant impact on block duration with AA-6 nanogels ($p > 0.10$ for all pair-wise comparisons). For AA-20 nanogels, smaller nanogels prolonged the duration of block to a greater extent than larger nanogels ($p = 0.03$ comparing AA-20L and AA-20S). In contrast, for the AA-33 nanogels, smaller particles facilitated shorter nerve blocks than larger particles ($p = 0.002$). It should be noted that the nanogel residue associated with AA-20L injections was a liquid-like, free-flowing suspension while AA-33L exhibited a gel-like residue, suggesting different interparticle interactions may occur between the two different nanogels *in vivo*.

To attempt to generate longer durations of block, experiments were conducted in which higher concentrations of bupivacaine were loaded into nanogels and compared to the durations of block from bupivacaine solutions without nanogels (Table 3). As shown in previous work[36], the injection of higher concentrations of bupivacaine solution increased the duration of nerve block, although non-linear increases in nerve block duration are observed with the concentration of anesthetic administered (Table 3). Co-injection of AA-6M prolonged the duration of nerve block by ~80 minutes relative to bupivacaine alone regardless of the total concentration of bupivacaine loaded into the nanogels. In contrast, co-injection of AA-33M induced a ~1.5 hour prolongation of nerve blockade in the presence of 5 mg/mL bupivacine and a much longer ~4.5 hour prolongation in the presence of 15 mg/mL bupivacaine relative to the drug solutions alone. Thus, nanogels with higher concentrations of acid functional groups (i.e. higher concentrations of ionic binding sites for bupivacaine) facilitated longer nerve blocks when loaded with higher concentrations of bupivacaine, while less functionalized nanogels with fewer ionic binding sites did not demonstrate this trend.

Nanogel concentration could also be modified to tune the duration of drug release and thus the duration of nerve block, as shown in Figure 5. In general, slower drug release (and thus prolonged anesthesia) would be expected as the nanogel concentration increased, given that a higher number of bupivacaine binding sites would be available. AA-20S nanogels followed this trend, with the duration of nerve block increasing linearly with the concentration of nanogel added up to 160 mg/mL nanogel concentration ($R^2 = 0.98$). AA-20L nanogels showed a similar linear correlation between nanogel concentration and nerve block duration up to 80 mg/mL nanogel ($R^2 = 0.92$) but then exhibited a decrease in the duration of effective nerve block at higher nanogel concentrations. A similar trend was observed for AA-33M, with the observed decrease in nerve block duration occurring at nanogel concentrations above 40 mg/mL. This curve shape suggests that drug release becomes sufficiently slow at higher nanogel concentrations that it falls below the minimum rate of drug release required for anesthesia.

4. DISCUSSION

Nanogels are attractive materials for drug delivery given that their size, porosity, and bulk and surface compositions can be well-controlled by tuning the synthesis procedure. This is particularly true for the delivery of charged drugs, since the nanogel can be designed to have optimized ionic (and/or hydrophobic) partitioning affinities specific to a particular drug. Acid-functionalized poly(N-isopropylacrylamide)-based nanogels are specifically useful for the controlled release of bupivacaine given the ionic attractions between the anionic charges on the nanogels and cationic bupivacaine molecules. This effect facilitates both higher-capacity loading of bupivacaine into the nanogel phase via ion exchange and slower release of bupivacaine release from the nanogel phase via diffusion, prolonging drug delivery rates and thus the clinical effectiveness of bupivacaine and other anesthetics. The acrylic acid-functionalized nanogels primarily used in this study are particularly useful in that copolymerization kinetics impart a relatively uniform distribution of anionic AA residues throughout the nanogel[20], facilitating improved cationic drug binding relative to more surface-functionalized nanogels[31].

Smaller (<300 nm) nanogels induced only mild inflammatory responses and cytotoxicity, while larger (>800 nm) nanogels induced slightly higher toxicity in cell culture and significantly more severe tissue responses, with thick, highly vascularized inflammatory capsules forming around the injected nanogel suspension and inflammation occurring deep within adjacent muscle tissue. Large and small nanogels may interact differently with macrophages[37] or be partitioned within the body by a different pathway, contributing to the different inflammatory response observed. For example, it is known that smaller particles are more likely to leave the site of injection than are larger ones[38]; they usually are then distributed to the reticulondothelal system, particularly the liver and spleen.

It is well-known that PNIPAM-based nanogels are prone to aggregation at temperatures above their volume phase transition temperature in high-salt environments such as the body, given that the nanogels are predominantly electrostatically stabilized following a phase transition and the high local salt concentration results in charge screening[39]. The potential occurrence of thermoaggregation for some nanogels but not others was therefore investigated as a possible explanation for the different tissue responses observed through *in vitro* aggregation experiments and the different durations of anesthesia achieved. Figure 6 shows *in vitro* measurements of AA-6 nanogel stability in saline solutions with and without the addition of 0.1mM bovine serum albumin. This solution mimics both the total protein concentration in the interstitial fluid environment of the injection site and the ionic strength and pH of the injected nanogel suspensions. Both in the presence and absence of protein, AA-6S nanogels aggregated at lower temperatures than AA-6L nanogels, presumably due to

the higher surface area-to-volume ratio (and thus larger driving force for surface area reduction via particle aggregation) of smaller nanogels. When protein was added, protein adsorption to the nanogel surface increased the aggregation temperature such that the aggregation temperature of the AA-6L nanogels was above physiological temperature while the aggregation temperature of both AA-6M and AA-6S nanogels remained below physiological temperature. Correspondingly, a free-flowing suspension was recovered inside the inflammation complex formed following *in vivo* injection of AA-6L nanogels while a gel-like aggregate (with similar mechanical and optical properties to the aggregates formed in the *in vitro* experiment) was observed following AA-6M injections (Fig. 2). *In vitro* aggregation measurements similarly predicted whether a free-flowing suspension or a gel-like aggregate was recovered from the injection site upon injection of both AA-20 nanogels (Fig. 3 and Supplementary Data, Figure S4) and AA-33 nanogels (Supplementary Figures S3 and S5); larger nanogels and nanogels with lower acid contents aggregated at higher temperatures, consistent with the *in vivo* observations of nanogel residues.

The phenomenon of nanogel thermoaggregation *in vivo* may also explain drug release kinetics that were not consistent with predictions based on simple diffusional path length or drug affinity arguments. As the net anionic charge density of the nanogel increases (i.e. at higher degrees of acrylic acid functionalization), more ionic bupivacaine binding sites are present; as a result, more bupivacaine bound to the nanogel and the overall rate of bupivacaine release was reduced. In cases in which the nanogels are more likely to aggregate upon injection (i.e. smaller and more highly acid-functionalized nanogels, Fig. 6 and Supplementary Figures S4 and S5), the fabrication of a macroscopic aggregate from a nanoscopic nanogel increases the average diffusional path length for drug release from the nanogel, thus reducing the bupivacaine release rate relative to what would be predicted based on the nanogel particle size alone. However, if the drug affinity / binding capacity or diffusional path length is too high, drug release can be slowed below the clinically effective dose of bupivacaine to maintain anesthesia, resulting in a shorter duration of effective block in these systems even though the actual rate of drug release is slower.

These diffusional and drug affinity arguments can be used to rationalize the release results observed for nanogels with varying sizes and varying degrees of functionalization. Note that bupivacaine was not explicitly loaded into the nanogel phase in this work; a total of 1.5 mg of bupivacaine was present in each injection, with drug partitioned between the PBS solution and nanogel phases based on the affinity of bupivacaine for the nanogel. At low degrees of functionalization (AA-6), relatively few ionic binding sites were present inside the nanogels such that a greater proportion of the bupivacaine present was in the bulk solution. As a result, irrespective of whether thermoaggregation occurred or not, the majority of bupivacaine was not loaded into the nanogel phase in AA-6 nanogels and thus nanogel size and/or aggregation state had no significant impact on the duration of effective block achieved (Table 2). It should be noted however that a significant prolongation in nerve block was still observed for all AA-6 nanogels relative to a bupivacaine-only injection ($p < 0.005$), due to the fraction of bupivacaine that did bind to the nanogel phase (Table 2). Similarly, no significant increase in nanogel-related nerve block prolongation was observed when the bupivacaine concentration was increased from 5 mg/mL to 15 mg/mL, with the addition of nanogel increasing the block duration by an equivalent ~80 minutes relative to the corresponding bupivacaine-only injection at both tested bupivacaine concentrations (Table 3).

At intermediate degrees of functionalization (AA-20), more ionic binding sites were present and a greater fraction of bupivacaine was loaded into the nanogel phase. As a result, if nanogels aggregated, the effective diffusional path length for drug release would be significantly larger, resulting in a slower overall drug release rate and a prolonged duration

of anesthesia. Correspondingly, nanogels that exhibited residues upon dissection and lower aggregation temperatures in the *in vitro* assay (AA-20M and AA-20S) facilitated longer nerve blocks than nanogels in which liquid-like residues were recovered following injection and which exhibited higher aggregation temperatures in the *in vitro* assay (AA-20L, Table 2).

At high degrees of functionalization (AA-33), the nanogel phase had the highest affinity for cationic bupivacaine, resulting in significant slowing of drug release due to partitioning of a large fraction of added bupivacaine into the nanogel phase. In this case, the combined effects of the high nanogel-drug affinity and the longer average diffusional path length resulting from potential nanogel thermoaggregation (gel-like residues were observed following dissection for both AA-33 nanogels tested) reduced the rate of bupivacaine release to such a degree that the dose delivered was below the effective dose for anesthesia. As a result, the drug release rate in AA-33M remained in the effective clinical window for a shorter period of time than with nanogels containing lower acid contents; consequently, AA-33M yielded a shorter duration of anesthesia than AA-20M (Table 2). When the bupivacaine concentration was increased from 5 mg/mL to 15 mg/mL, the large excess of $-COO^-$ binding sites for available bupivacaine in the highly functionalized AA-33 nanogels (5-fold excess even at the higher bupivacaine concentration tested) facilitated significantly higher overall drug loading into the nanogel phase. Consequently, a larger overall larger concentration gradient existed to drive drug release from the nanogels and the overall mass of drug released per unit time was increased. Correspondingly, the observed duration of nerve block increased by a factor of three as the loading concentration of bupivacaine increased from 5 mg/mL to 15 mg/mL (i.e. anesthetic release could be sustained in the clinical window for a longer period of time than was possible in nanogels loaded with less drug).

The observed nanogel concentration effects can similarly be rationalized based on the combined effects of drug affinity and nanogel aggregation. As more nanogel was added, more bupivacaine could bind to the nanogel phase, resulting in slower drug release. For nanogels with high concentrations of bupivacaine binding sites (AA-33), increasing the nanogel concentration from 40 mg/mL to 80 mg/mL increased the fraction of total bupivacaine bound and thus slowed bupivacaine release to the point that the release rate was lower than that required to maintain clinical anesthesia; as a result, a decrease in nerve block duration was observed (Fig. 5). A similar trend was observed for AA-20L, although the observed decrease in nerve block duration occurred at higher nanogel concentrations than in AA-33M due to the lower total functional group content (and thus lower bupivacaine binding capacity) of AA-20L nanogels. It should be noted that the observed decrease in block duration with AA-20L also coincided with the conversion of the nanogel residue after four days of injection from a free-flowing liquid at lower nanogel concentrations to a gel-like residue at higher nanogel concentrations. This observation suggests that the spontaneous thermogelation of the nanogel (and the corresponding increase in effective diffusional path length to drug release) at concentrations greater than 120 mg/mL may also contribute to the shorter duration of anesthesia achieved. We expect a similar trend to occur in AA-20S at higher gel loadings, but could not test these higher concentrations due to the very high viscosity of such systems that made injection through a 25G needle impractical.

Bupivacaine-loaded nanogels provided durations of nerve block which compare favorably with other drug delivery systems and, in particular, other *in situ*-gelling hydrogel-based systems previously studied. Block durations up to 5 hours were achieved using polysaccharide-based rheological blends[40] and 2.5 hours using an *in situ*-gelling hyaluronic acid-based hydrogel[14] to deliver bupivacaine; a 5 hour block was achieved using a thermally-gelling Pluronic copolymer to deliver lidocaine[41]. In comparison,

AA-20S nanogels at high concentrations (160mg/mL) provided block durations up to 8–9 hours. This block duration is comparable to that achieved using lipid-protein-sugar microparticles (~5 hours)[42] and PLGA microparticles (~8 hours)[7]. Furthermore, administration of nanogels avoids the long-duration inflammatory foreign body response observed when PLGA microparticles are used as the delivery vehicle[43]. However, the nanogels used in this paper are not biodegradable through an obvious mechanism as synthesized here (via free radical copolymerization). Nonetheless, this work provides proof-of-concept of the value of nanogels with these properties for the delivery of local anesthetics and cationic drugs in general.

5. CONCLUSIONS

Acid-functionalized poly(N-isopropylacrylamide)-based nanogels are useful as drug delivery vehicles for the delivery of local anesthetics. Acid-functionalized nanogels had high affinity for bupivacaine via ionic partitioning, permitting efficient drug loading and release using nanogel delivery vehicles. Cytotoxicity studies indicated that nanogels had a minimal impact on the viability of myoblasts, fibroblasts, and macrophages *in vitro.* Large (~800–1000 nm) acid-functionalized nanogels provided moderate durations of nerve block (~5–6 hours) which were comparable to those from previous hydrogel-based systems. However, large nanogels also induced an extensive inflammatory response in which a thick inflammatory capsule formed around the injected nanogel suspension. In contrast, small acid-functionalized nanogels resulted in durations of sciatic nerve blockade of up to ~8–9 hours while inducing only a mild inflammatory response. Drug release kinetics can be rationalized based on the relative affinities of different nanogels for bupivacaine and the potential thermoaggregation of some nanogels upon injection to create a macroscopic drug release vehicle. On this basis, nanogels are potentially attractive vehicles for prolonged local anesthesia.

Supplementary Material

Refer to Web version on PubMed Central for supplementary material.

Acknowledgments

DSK acknowledges NIH GM073626 and TH acknowledges the Natural Sciences and Engineering Research Council of Canada (NSERC) for research funding. SY acknowledges the NSERC Undergraduate Student Research Award for funding.

References

1. Masters DB, Berde CB, Dutta SK, Griggs CT, Hu D, Kupsky W, et al. Prolonged Regional Nerve Blockade by Controlled-Release of Local-Anesthetic from a Biodegradable Polymer Matrix. Anesthesiology. 1993; 79:340–6. [PubMed: 8342843]
2. Sendil D, Wise DL, Hasirci V. Assessment of biodegradable controlled release rod systems for pain relief applications. J Biomat Sci-Polym E. 2002; 13:1–15.
3. Masters DB, Domb AJ. Liposphere local anesthetic timed-release for perineural site application. Pharmaceut Res. 1998; 15:1038–45.
4. Cereda CMS, De Araujo DR, Brunetto GB, De Paula E. Liposomal prilocaine: preparation, characterization, and in vivo evaluation. J Pharm Pharm Sci. 2004; 7:235–40. [PubMed: 15367381]
5. Epstein-Barash H, Shichor I, Kwon AH, Hall S, Lawlor MW, Langer R, et al. Prolonged duration local anesthesia with minimal toxicity. P Natl Acad Sci USA. 2009; 106:7125–30.
6. Lecorre P, Leguevello P, Gajan V, Chevanne F, Leverge R. Preparation and Characterization of Bupivacaine-Loaded Polylactide and Polylactide-Co-Glycolide Microspheres. Int J Pharm. 1994; 107:41–9.

7. Curley J, Castillo J, Hotz J, Uezono M, Hernandez S, Lim JO, et al. Prolonged regional nerve blockade - Injectable biodegradable bupivacaine/polyester microspheres. Anesthesiology. 1996; 84:1401–10. [PubMed: 8669682]
8. Bernardo MV, Blanco MD, Gomez C, Olmo R, Teijon JM. In vitro controlled release of bupivacaine from albumin microspheres and a co-matrix formed by microspheres in a poly(lactide-co-glycolide) film. J Microencapsul. 2000; 17:721–31. [PubMed: 11063419]
9. Kohane DS, Lipp M, Kinney RC, Lotan N, Langer R. Sciatic nerve blockade with lipid-protein-sugar particles containing bupivacaine. Pharmaceut Res. 2000; 17:1243–9.
10. Kohane DS, Smith SE, Louis DN, Colombo G, Ghoroghchian P, Hunfeld NGM, et al. Prolonged duration local anesthesia from tetrodotoxin-enhanced local anesthetic microspheres. Pain. 2003; 104:415–21. [PubMed: 12855352]
11. Xu QB, Hashimoto M, Dang TT, Hoare T, Kohane DS, Whitesides GM, et al. Preparation of Monodisperse Biodegradable Polymer Microparticles Using a Microfluidic Flow-Focusing Device for Controlled Drug Delivery. Small. 2009; 5:1575–81. [PubMed: 19296563]
12. Bernardo MV, Blanco MD, Olmo R, Teijon JM. Delivery of bupivacaine included in poly(acrylamide-co-monomethyl itaconate) hydrogels as a function of the pH swelling medium. J Appl Polym Sci. 2002; 86:327–34.
13. Blanco MD, Bernardo MV, Teijon C, Sastre RL, Teijon JM. Transdermal application of bupivacaine-loaded poly (acrylamide(A)-co-monomethyl itaconate) hydrogels. Int J Pharm. 2003; 255:99–107. [PubMed: 12672606]
14. Jia XQ, Colombo G, Padera R, Langer R, Kohane DS. Prolongation of sciatic nerve blockade by in situ cross-linked hyaluronic acid. Biomaterials. 2004; 25:4797–804. [PubMed: 15120526]
15. Shamji MF, Whitlatch L, Friedman AH, Richardson WJ, Chilkoti A, Setton LA. An injectable and in situ-gelling biopolymer for sustained drug release following perineural administration. Spine. 2008; 33:748–54. [PubMed: 18379401]
16. Dollo G, Malinovsky JM, Peron A, Chevanne F, Pinaud M, Le Verge R, et al. Prolongation of epidural bupivacaine effects with hyaluronic acid in rabbits. Int J Pharm. 2004; 272:109–19. [PubMed: 15019074]
17. Gianolio DA, Philbrook M, Avila LZ, MacGregor H, Duan SX, Bernasconi R, et al. Synthesis and evaluation of hydrolyzable hyaluronan-tethered bupivacaine delivery systems. Bioconjugate Chem. 2005; 16:1512–8.
18. Lagarce F, Faisant N, Desfontis JC, Marescaux L, Gautier F, Richard J, et al. Baclofen-loaded microspheres in gel suspensions for intrathecal drug delivery: In vitro and in vivo evaluation. Eur J Pharm Biopharm. 2005; 61:171–80. [PubMed: 15967653]
19. Blanco MD, Bernardo MV, Gomez C, Muniz E, Teijon JM. Bupivacaine-loaded comatrix formed by albumin microspheres included in a poly(lactide-co-glycolide) film: in vivo biocompatibility and drug release studies. Biomaterials. 1999; 20:1919–24. [PubMed: 10514068]
20. Hoare T, McLean D. Kinetic prediction of functional group distributions in thermosensitive microgels. J Phys Chem B. 2006; 110:20327–36. [PubMed: 17034214]
21. Routh AF, Vincent B. Salt-induced homoaggregation of poly(N-isopropylacrylamide) microgels. Langmuir. 2002; 18:5366–9.
22. Snowden, MJ.; Booty, MT.; Karsa, D. Encapsulation and Controlled Release. London: Royal Society of Chemistry; 1993.
23. Snowden MJ. The Use of Poly(N-Isopropylacrylamide) Lattices as Novel Release Systems. J Chem Soc-Chem Comm. 1992:803–4.
24. Nolan CM, Gelbaum LT, Lyon LA. H-1 NMR investigation of thermally triggered insulin release from poly(N-isopropylacrylamide) microgels. Biomacromolecules. 2006; 7:2918–22. [PubMed: 17025370]
25. Huo DX, Li YN, Qian QW, Kobayashi T. Temperature-pH sensitivity of bovine serum albumin protein-microgels based on cross-linked poly(N-isopropylacrylamide-co-acrylic acid). Colloid Surface B. 2006; 50:36–42.
26. Serpe MJ, Yarmey KA, Nolan CM, Lyon LA. Doxorubicin uptake and release from microgel thin films. Biomacromolecules. 2005; 6:408–13. [PubMed: 15638546]

27. Nolan CM, Serpe MJ, Lyon LA. Thermally modulated insulin release from microgel thin films. Biomacromolecules. 2004; 5:1940–6. [PubMed: 15360309]
28. Cornelius, VJ.; Mitchell, JC.; Snowden, MJ. Application BP. United Kingdom: 2005.
29. Huang G, Gao J, Hu ZB, John JVS, Ponder BC, Moro D. Controlled drug release from hydrogel nanoparticle networks. J Controlled Release. 2004; 94:303–11.
30. Eichenbaum GM, Kiser PF, Dobrynin AV, Simon SA, Needham D. Investigation of the swelling response and loading of ionic microgels with drugs and proteins: The dependence on cross-link density. Macromolecules. 1999; 32:4867–78.
31. Hoare T, Pelton R. Impact of microgel morphology on functionalized microgel-drug interactions. Langmuir. 2008; 24:1005–12. [PubMed: 18179266]
32. Hoare, T.; Sivakumaran, D.; Stefanescu, CF.; Lawlor, MW.; Kohane, DS. Nanogel scavengers for drugs: Local anesthetic uptake by thermoresponsive nanogels. Acta Biomaterialia. 2011. http://dx.doi.org/10.1016/j.actbio.2011.12.028in press
33. Thalhammer JG, Vladimirova M, Bershadsky B, Strichartz GR. Neurologic Evaluation of the Rat during Sciatic-Nerve Block with Lidocaine. Anesthesiology. 1995; 82:1013–25. [PubMed: 7717536]
34. Fogh-Andersen N, Altura BM, Altura BT, Siggaard-Andersen O. Composition of Interstitial Fluid. Clin Chem. 1995; 41:1522–5. [PubMed: 7586528]
35. Kohane DS, Lipp M, Kinney RC, Anthony DC, Louis DN, Lotan N, et al. Biocompatibility of lipid-protein-sugar particles containing bupivacaine in the epineurium. J Biomed Mater Res. 2002; 59:450–9. [PubMed: 11774302]
36. Grant GJ, Vermeulen K, Zakowski MI, Sutin KM, Ramanathan S, Langerman L, et al. A Rat Sciatic-Nerve Model for Independent Assessment of Sensory and Motor Block Induced by Local-Anesthetics. Anesth Analg. 1992; 75:889–94. [PubMed: 1443707]
37. He C, Hu Y, Yin L, Tang C, Yin C. Effects of particle size and surface charge on cellular uptake and biodistribution of polymeric nanoparticles. Biomaterials. 2010; 31:3657–66. [PubMed: 20138662]
38. Kohane DS, Tse J, Yeo Y, Padera R, Shubina M, Langer R. Biodegradable polymeric microspheres and nanospheres for drug delivery in the peritoneum. J Biomed Mater Res A. 2006; 77A:351–61. [PubMed: 16425240]
39. Makino K, Kado H, Ohshima H. Aggregation behavior of poly(N-isopropylacrylamide) microspheres. Colloid Surface B. 2001; 20:347–53.
40. Hoare T, Bellas E, Zurakowski D, Kohane DS. Rheological blends for drug delivery. II: Prolongation of nerve blockade, biocompatibility, and in vitro-in vivo correlations. J Biomed Mater Res Part A. 2008; 92A:586–595.
41. Chen PC, Kohane DS, Park YJ, Bartlett RH, Langer R, Yang VC. Injectable microparticle-gel system for prolonged and localized lidocaine release. II. In vivo anesthetic effects. J Biomed Mater Res A. 2004; 70A:459–66. [PubMed: 15293320]
42. Colombo G, Langer R, Kohane DS. Effect of excipient composition on the biocompatibility of bupivacaine-containing microparticles at the sciatic nerve. J Biomed Mater Res A. 2004; 68A: 651–9. [PubMed: 14986320]
43. Kohane DS, Lipp M, Kinney RC, Anthony DC, Louis DN, Lotan N, et al. Biocompatibility of lipid-protein-sugar particles containing bupivacaine in the epineurium. J Biomed Mater Res. 2002; 59:450–9. [PubMed: 11774302]

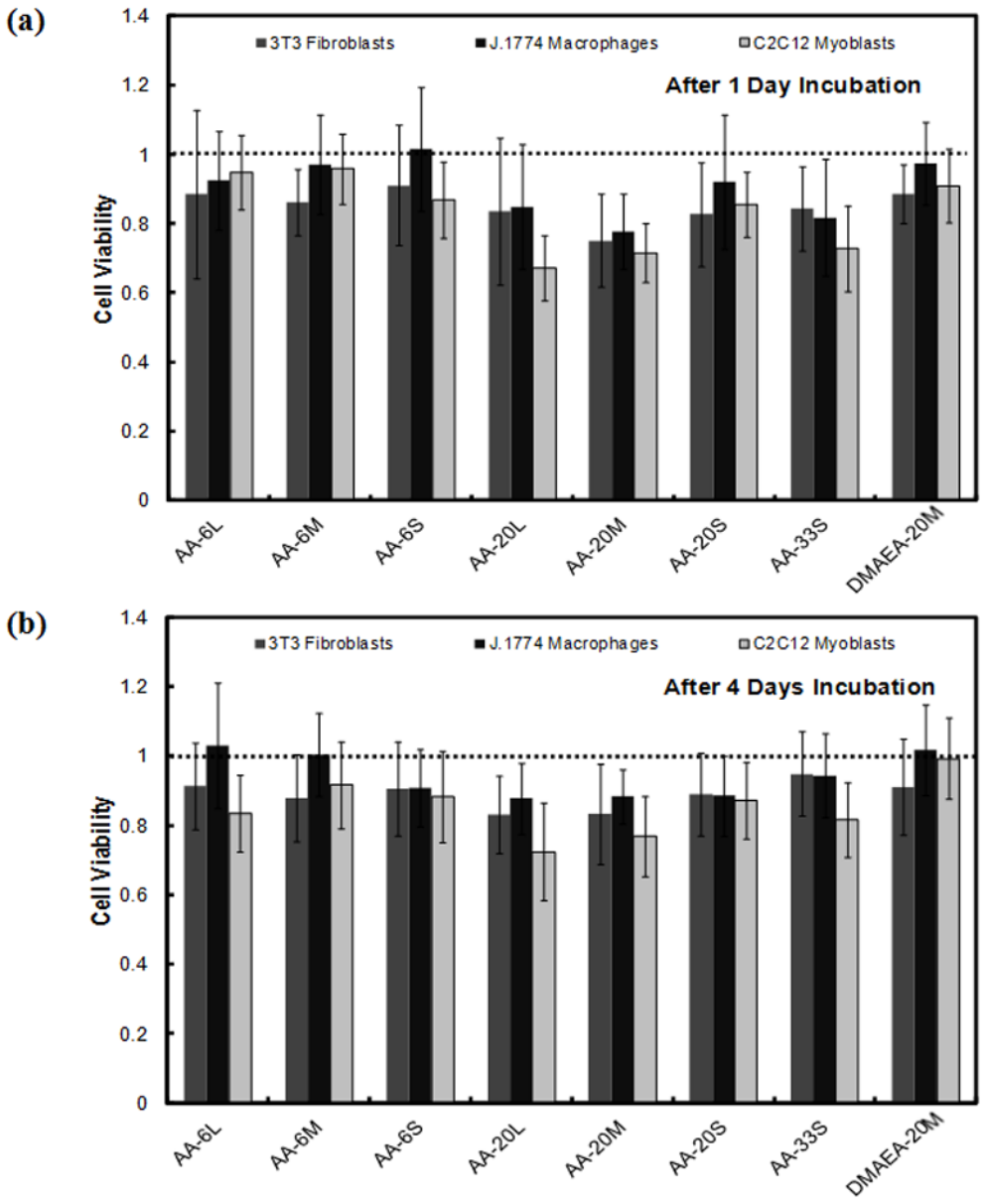

Figure 1.

Cell viability (expressed as a ratio to viability of cells not exposed to particles) of 3T3 fibroblasts, J1774 macrophages, and C2C12 myoblasts in the presence of 2 mg/mL of nanogels after (a) 1 day and (b) 4 days of incubation. The dotted line represents cell viability in the absence of nanogels. Data are means ± standard deviation ($n = 4$).

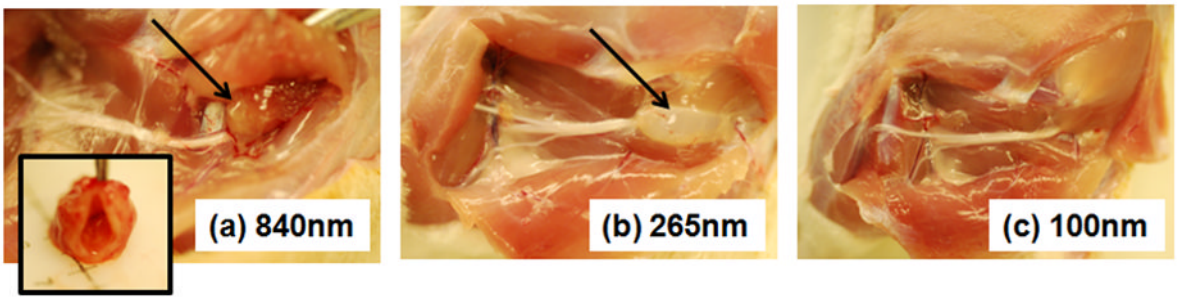

Figure 2.
Tissue response after 4 days to injection of AA-6 nanogels of different sizes at the sciatic nerve (a) AA-6L, particle size = 840 nm; (b) AA-6M, particle size = 265 nm; (c) AA-6S, particle size = 100 nm. Arrows point to the residual nanogel deposit/inflammatory complex. The inset to (a) is the cross-section of the inflammatory capsule shown in panel (a).

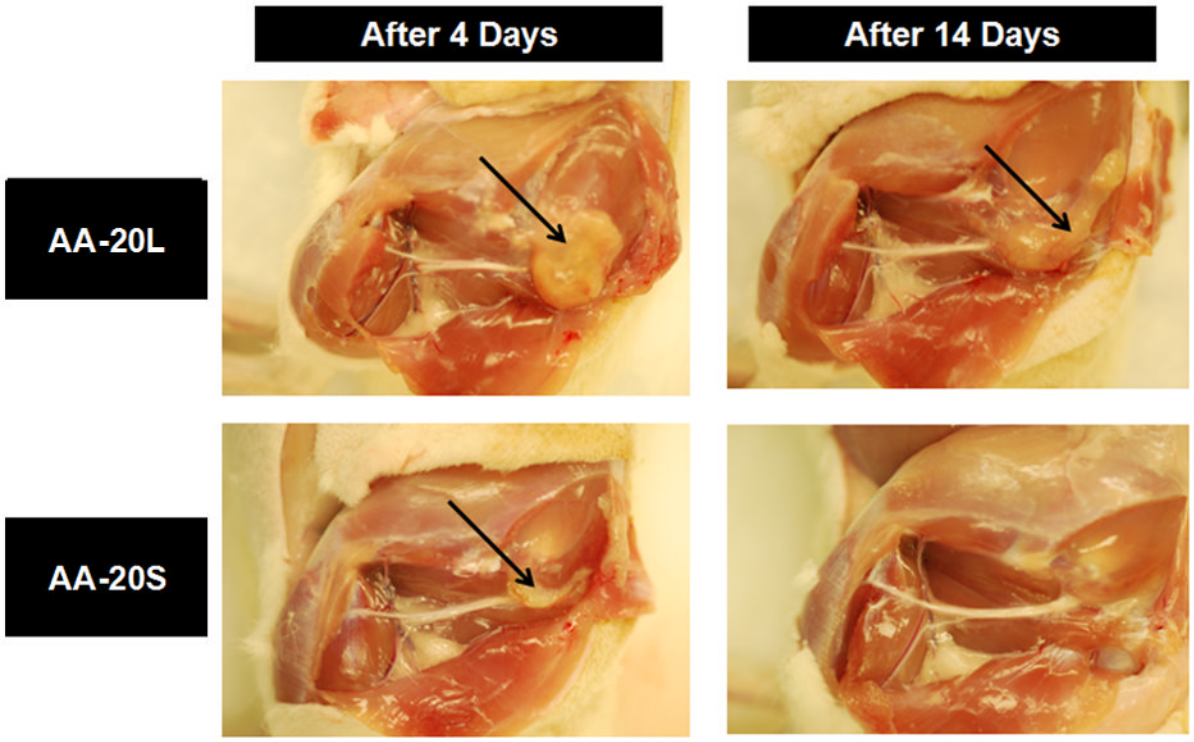

Figure 3.
Tissue response to sciatic nerve injection of AA-20L (particle size = 815 nm) and AA-20S (particle size = 170 nm) nanogels, four and fourteen days after injection. Arrows point to the residual nanogel deposit and/or inflammatory complex.

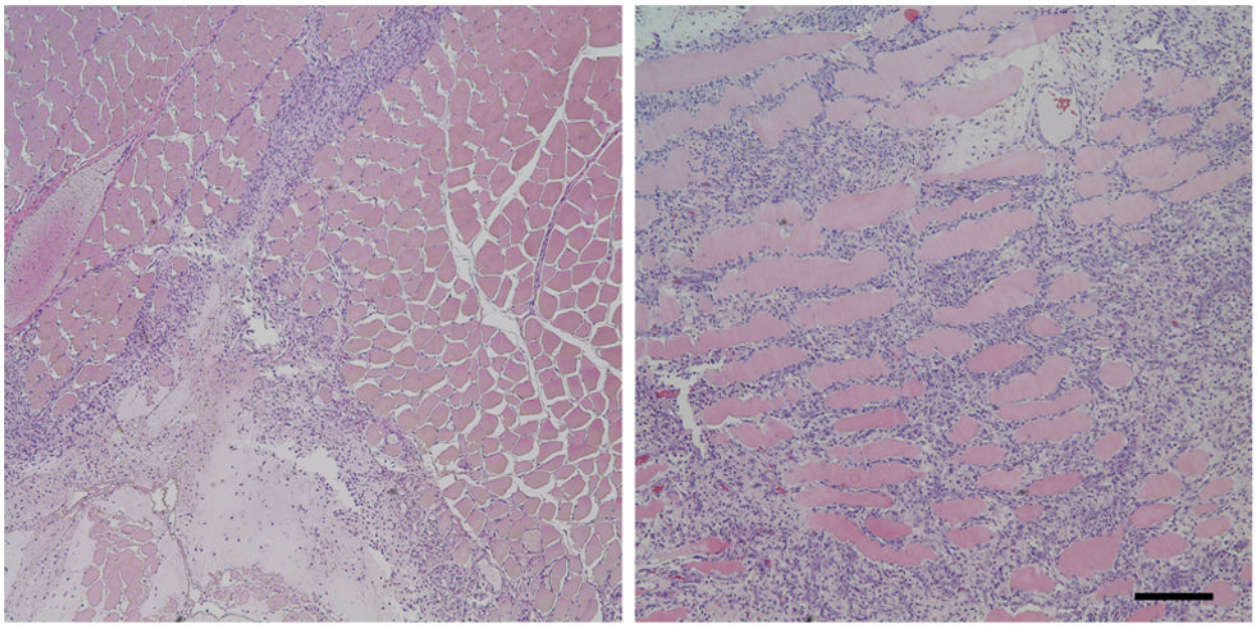

Figure 4.
Histological findings on hematoxylin-eosin stained sections 4 days after injection of AA-20S (Fig. 4a) and AA-20L (Fig. 4b) nanogels. An inflammatory reaction consisting of lymphocytes and macrophages was elicited with both types of nanogel, but the degree of inflammation (area with dense blue nuclei) was much greater for AA-20L. Bar = 200 μm.

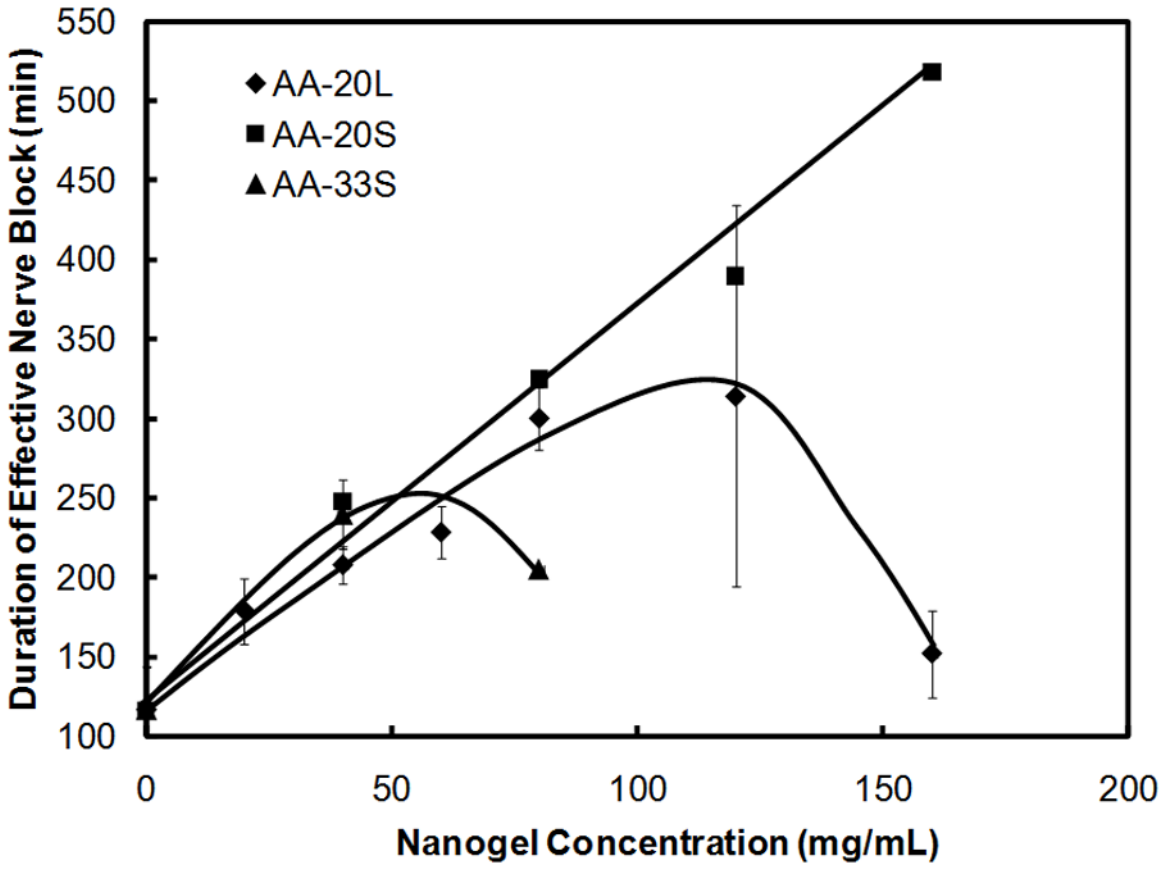

Figure 5.
Duration of sensory nerve block as a function of nanogel concentration and acid functionalization; 5 mg/mL total bupivacaine ($n = 4$)

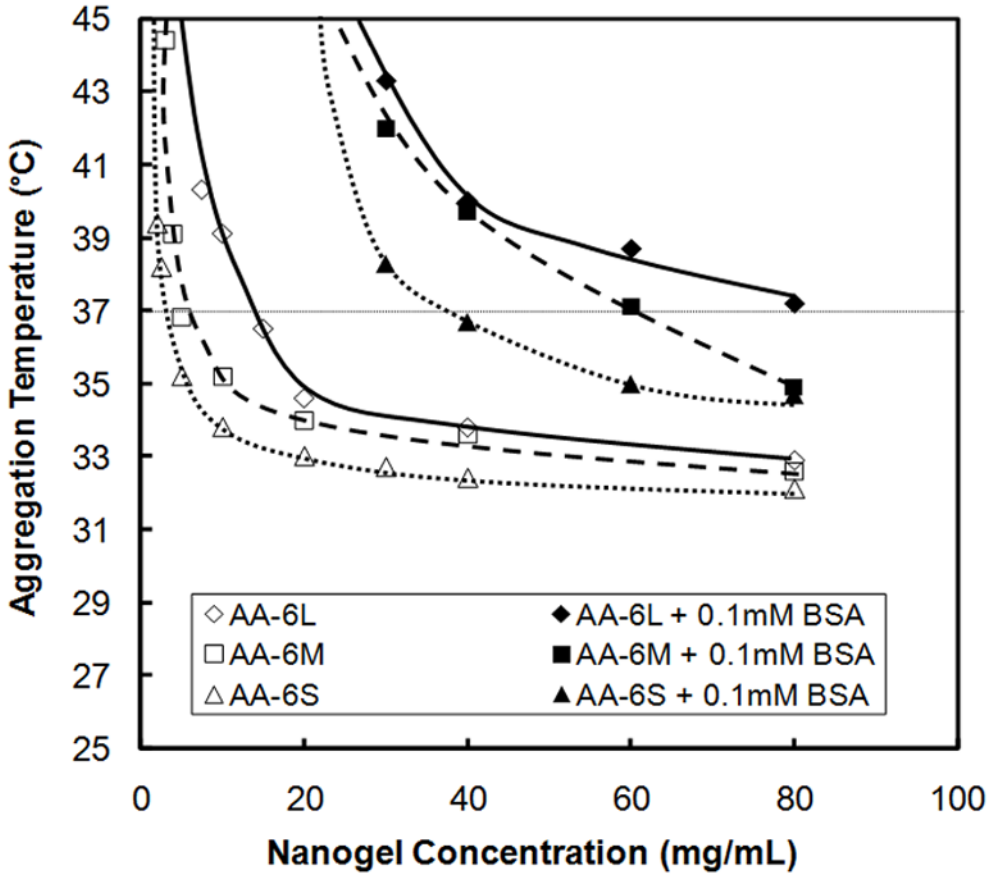

Figure 6.
Critical aggregation temperature of AA-6 nanogels with varying sizes measured in saline (0.15M NaCl) in the absence and presence of 0.1 mM bovine serum albumin (BSA), representative of the total protein concentration in interstitial fluid ($n = 4$)

Table 1

Nanogel recipes and physical properties

Nanogel	NIPAM (g)	AA (g)	DMAEA (g)	BIS (g)	SDS (g)	Functional Monomer Loading[a] (mol%, theory)	Functional Monomer Incorporation[b] (% theoretical)	Particle Size (nm)	Electrophoretic Mobility ($x10^{-8}$ m^2/Vs)
AA-6L	1.4	0.058	0	0.10	0	5.8	96 ± 8	840 ± 28	−0.92 ± 0.05
AA-6M	1.4	0.058	0	0.10	0.05	5.8	95 ± 8	265 ± 1	−0.78 ± 0.06
AA-6S	1.4	0.058	0	0.10	0.20	5.8	94 ± 7	110 ± 1	−0.77 ± 0.10
AA-20L	1.4	0.232	0	0.10	0	19.8	96 ± 3	974 ± 16	−1.98 ± 0.08
AA-20M	1.4	0.232	0	0.10	0.05	19.8	94 ± 5	458 ± 3	−1.12 ± 0.12
AA-20S	1.4	0.232	0	0.10	0.20	19.8	97 ± 4	198 ± 7	−0.73 ± 0.07
AA-33L	1.4	0.464	0	0.10	0	33.1	92 ± 5	1029 ± 77	−1.56 ± 0.06
AA-33M	1.4	0.464	0	0.10	0.30	33.1	95 ± 6	287 ± 4	−1.64 ± 0.08
DMAEA-20S	1.4	0	0.504	0.10	0	19.8	N/A	216 ± 2	−0.46 ± 0.06

[a] mol% of functional monomer (relative to total monomer content of nanogel) in recipe

[b] % of theoretical functional monomer loading achieved in nanogel product (as measured via conductometric titration)

Table 2

Duration of sensory and motor nerve blocks from sciatic nerve injection of nanogel suspensions (80 mg/mL) loaded with in 5 mg/mL bupivacaine ($n = 4$). Corresponding thermoaggregation temperature (as measured in saline with 0.1mM bovine serum albumin added) at 80 mg/mL nanogel concentration are also shown ($n = 4$).

Nanogel	Latency Nerve Block (min)	Motor Nerve Block (min)	Thermoaggregation Temperature (°C, saline+0.1mM BSA)
No Nanogel	117 ± 27	119 ± 21	N/A
DMAEA-20	139 ± 25	159 ± 17	35.0
AA-6L	199 ± 36	203 ± 43	37.5
AA-6M	220 ± 26	222 ± 30	34.9
AA-6S	201 ± 27	213 ± 23	34.2
AA-20L	300 ± 20	309 ± 30	37.2
AA-20M	345 ± 41	365 ± 33	34.8
AA-20S	390 ± 84	409 ± 83	34.6
AA-33L	306 ± 25	318 ± 12	36.3
AA-33M	205 ± 1	210 ± 4	32.4

Table 3

Effect of bupivacaine concentration on the duration of nerve block in the absence of nanogels as well as in the presence of 80 mg/mL AA-6M and AA-33M nanogels ($n = 4$)

Bupivacaine Concentration (mg/mL)	Latency, No Nanogel (min)	AA-6M		AA-33M	
		Latency (min)	Nanogel Prolongation of Block (min)	Latency (min)	Nanogel Prolongation of Block (min)
5	117 ± 27	220 ± 26	103 ± 53	205 ± 1	88 ± 28
10	189 ± 7	266 ± 3	77 ± 10	393 ± 47	204 ± 54
15	206 ± 17	286 ± 14	80 ± 31	481 ± 38	275 ± 31